Journal of Rock Mechanics and Geotechnical Engineering 14 (2022) 1241–1252

Contents lists available at ScienceDirect

Journal of Rock Mechanics and Geotechnical Engineering

journal homepage: www.jrmge.cn

Full Length Article

Effect of fiber-reinforcement on the mechanical behavior of sand approaching the critical state

Jakhongirbek Ganiev [a,*], Shotaro Yamada [b], Masaki Nakano [a], Takayuki Sakai [a]

[a] Department of Civil Engineering, Nagoya University, Nagoya, 464-8603, Japan
[b] Department of Civil Engineering, Tohoku University, Sendai, 980-8579, Japan

ARTICLE INFO

Article history:
Received 14 May 2021
Received in revised form
25 August 2021
Accepted 18 October 2021
Available online 27 November 2021

Keywords:
Fiber-reinforced sand
Triaxial compression
Stress ratio
Critical state
Relative density

ABSTRACT

Several types of ground improvement methods that employ fiber-reinforcement have been developed in recent years. A series of consolidated drained triaxial compression tests has been conducted here to examine the effect of short fibers on the mechanical properties of Toyoura sand. Sand with 0%, 0.2%, 0.4%, and 1% fiber contents, prepared to yield random distribution, was sheared under several confining pressures and controlled via their initial relative densities. The test results showed that the maximum and residual deviatoric stresses increased, whereas the volumetric expansion decreased with an increase in fiber content. Although the stress ratio η $(=q/p')$ and specific volume changed depending on the fiber content and confining pressure with shear progression, they each reached the same values for a definite fiber content at the end of shearing, independent of initial relative density. In other words, the unique critical state line can be found for a definite fiber content. Moreover, the greater the fiber content, the larger the slope of the critical state line at the end of shearing. Additionally, as the length of fibers shortened with the same percentage of fiber inclusions in sand, the deviatoric stress and the stress ratio decreased, approaching the shear-strain-volumetric response of unreinforced sand.

1. Introduction

Fiber inclusions significantly improve the strength of soils; consequently, several types of ground improvement methods employing fiber-reinforcement have been developed in retaining structures, embankments and slopes, as well as for subgrade strengthening beneath footings and pavement. In order to evaluate the enhancement achieved through these methods, a constitutive model for fiber-reinforced soils and a numerical analysis code that underwrites the model have been desired.

The influence of flexible fibers on the shear strength and volumetric change behavior of soils has been investigated through direct shear (Gray and Ohashi, 1983; Jewell and Wroth, 1987; Yetimoglu and Salbas, 2003; Ibraim and Fourmont, 2006; Sadek et al., 2010; Falorca and Pinto, 2011; Eldesouky et al., 2016; Muir Wood et al., 2016), conventional triaxial compression and extension under both drained and undrained conditions (Maher and Gray, 1990; Michalowski and Ĉermak, 2003; Consoli et al., 2007a, 2009; Chen, 2010; Diambra et al., 2010; Silva Dos Santos et al., 2010; Lirer et al., 2011; Ibraim et al., 2012), and bender element and ring shear tests (Heineck et al., 2005; Consoli et al., 2007b; Liu et al., 2011). According to previous studies (Michalowski and Ĉermak, 2003; Heineck et al., 2005; Sadek et al., 2010; Lirer et al., 2011; Ajayi et al., 2017; Gao and Huang, 2021), some typical outcomes were obtained: fiber-reinforced specimens exhibited an initial stiffness reduction with increase of the peak strength and an reduction in the post-peak strength loss related to the nature of the fibers and grain size of the host soil in drained triaxial tests; the impact of fibers on the dilatancy behavior of soils was also investigated, where decreased volumetric change with the increase in fiber content was observed. In contrast, in some other studies, volumetric change behavior was rendered more dilative by introducing fibers into the soil (Ibraim and Fourmont, 2006; Consoli et al., 2009; Diambra et al., 2010). Despite the existence of a relatively large number of laboratory studies, there are still discrepancies in the test results and challenges in fiber-reinforced specimen preparation, which inhibit wide-spread practical application of this alternative soil stabilization technique. Most previous experimental studies examined the effects of not only fiber content

* Corresponding author.
E-mail address: ganiev.jakhongirbek@j.mbox.nagoya-u.ac.jp (J. Ganiev).
Peer review under responsibility of Institute of Rock and Soil Mechanics, Chinese Academy of Sciences.

https://doi.org/10.1016/j.jrmge.2021.10.003

and length, but also confining pressure and relative density on the mechanical behavior of fiber-reinforced sand. They have presented valuable results. However, few studies have discussed the simultaneous changes in deviatoric stress q, mean effective stress p', and specific volume v until the end of shearing in the drained triaxial compression test and, focused on the critical state line of fiber-reinforced sand based on the critical state concept. It should be useful to interpret the shear behavior of fiber-reinforced sand based on the critical state concept to construct a constitutive model for describing fiber-reinforced sand.

The critical state concept (Roscoe et al., 1958; Schofield and Wroth, 1968; Atkinson and Bransby, 1978) is one of the most important and basic concepts for understanding the mechanical behavior of soil. This concept has contributed to the proposal of many constitutive models for describing soils. An idealized family of critical state lines from high plastic silty clays and clays to almost non-plastic silty sandy soils were shown through the concept (Schofield and Wroth, 1968). The critical state of sandy soil has been presented and discussed in previous studies (Roscoe and Burland, 1968; Atkinson and Bransby, 1978; Verdugo and Ishihara, 1996). However, studies that focused on the interpretation of the mechanical behavior of sand reinforced with fibers through the critical state framework have been limited (Silva Dos Santos et al., 2010). Furthermore, analysis of the experimental work has been limited regarding the influence of various parameters and testing conditions on the composite materials. In order to apply or expand the models based on critical state soil mechanics to fiber-reinforced soil, this study investigates the mechanical properties of fiber-reinforced sand, with particular attention to the critical state.

In the present study, a more suitable specimen preparation method was obtained by checking the mechanical behavior of specimens with high reproducibility of test results from the other four methods. Then, a drained triaxial compression test was carried out to investigate the effects of fiber content, confining pressure, initial relative density, and fiber length on the shear behavior of fiber-reinforced sand. In particular, the present study addressed deviatoric stress q, mean effective stress p' and specific volume v through the shear process and up to the end of the test, and focused on the effect of fiber content on the critical state line of fiber-reinforced sand.

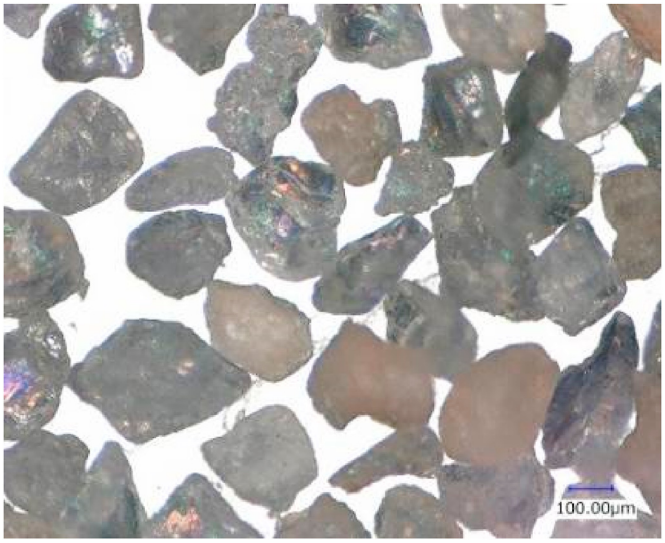

Fig. 1. Microscopic image of Toyoura sand.

2. Materials and methods

2.1. Materials

Toyoura sand, the standard sand for laboratory testing in Japan, was used for all the experiments. Toyoura sand is classified as clean and uniform fine sand (SP) in the Unified Soil Classification System (USCS), with sub-angular and angular shaped particles (Fig. 1). Its grain size distribution was obtained following the procedures specified in the Japanese standard JGS 0131–2015 (2015) (Fig. 2). The physical properties of the Toyoura sand are given in Table 1.

Polyvinyl alcohol (PVA) fibers have been used as a reinforcement material. A photograph of the fibers is shown in Fig. 3, and the main properties are summarized in Table 2.

2.2. Specimen preparation

Four fiber contents W_f i.e. 0%, 0.2%, 0.4% and 1%, were utilized to determine the correlation between the stress ratio and fiber content, and the evidence of fiber-reinforcement. The fiber content can be described as a mass ratio through the following equation:

$$W_f = \frac{m_f}{m_{sp}} \tag{1}$$

where m_f and m_{sp} are the masses of the fibers and soil particles, respectively.

The void ratio of fiber-reinforced sand is determined using the following equation, considering fibers as a part of solids (Michalowski and Čermak, 2003; Heineck et al., 2005; Silva Dos Santos et al., 2010):

$$e = \frac{V_v}{V_s} = \frac{V_a}{V_{sp} + V_f} \tag{2}$$

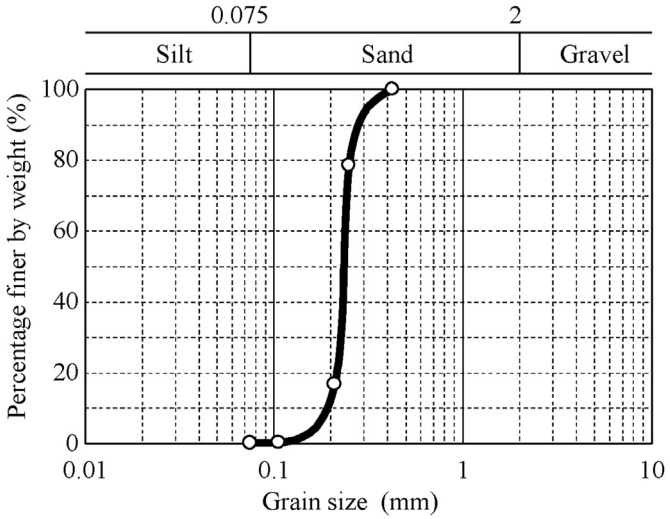

Fig. 2. Cumulative grain size distribution of Toyoura sand.

Table 1
Properties of Toyoura sand.

Specific gravity, G_s	Maximum void ratio, e_{max}	Minimum void ratio, e_{min}	Coefficient of uniformity, C_u	Coefficient of curvature, C_c
2.646	0.985	0.639	1560	41

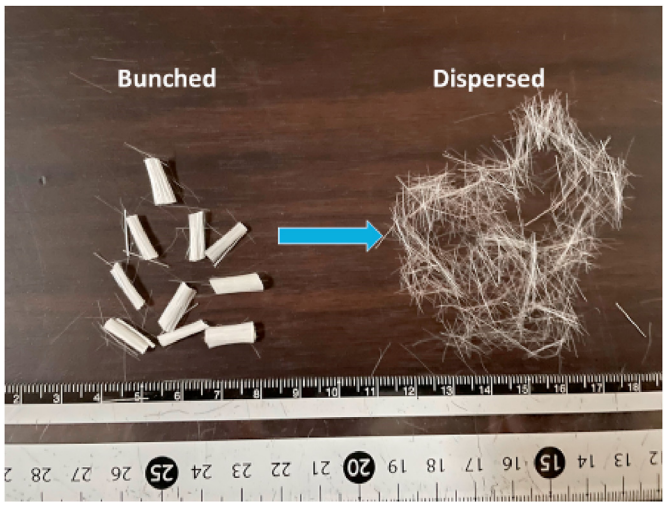

Fig. 3. Photograph of PVA fibers used in this study.

Table 2
Properties of the PVA fibers.

Length (mm)	Diameter (mm)	Specific gravity	Tensile strength (MPa)	Young's modulus (GPa)
12–15	0.04	1.3	1560	41

where V_a is the volume of air, V_f is the volume of the fibers, V_{sp} is the volume of soil particles, V_v is the volume of the voids, and V_s is the volume of solids.

The specimen preparation involved mixing fibers with sand and molding. Firstly, the fibers were weighed to achieve the desired percentage of fiber content. The fibers had to be manually dispersed from their bunched condition before being added to the sand, as seen in Fig. 3. First, a small amount of fiber was allocated and placed on the plate and covered with a layer of sand. This procedure was then repeated until all fibers and all of the sand had been added, forming a "sandwich". The mixing was determined through a trial-and-error method to obtain shear behavior with high reproducibility among four considered methods (Fig. 4):

(1) Manual mixing with a scoop in a dry condition, similar to mixing of two different sized granular soils;
(2) Manual mixing with a scoop at 10% water content;
(3) Automatic mixing using an electrical mixer in a dry condition; and
(4) Automatic mixing using an electrical mixer at 10% water content.

As can be seen from Fig. 4a, manual mixing in a dry condition was sufficient for homogenization of the admixture (sand + fiber) with low percentages of fiber inclusions (0.2% and 0.4%). Manual mixing of fibers with sand in a moist condition was also uniform enough. However, it was decided to compact the admixture into the mold by dry deposition identically with pure sand specimens. Once the percentage of reinforcing material increased to 1%, the segregation of sand and fiber was revealed (Fig. 4c), which required the addition of water (10% of moisture content) and the change of manual mixing to automatic mixing.

Once the fiber–sand mixtures appeared to be visually uniform, these masses were molded into a split mold with dimensions of 100 mm in height and 50 mm in diameter. An initial relative density D_r was obtained according to the following equation:

Fig. 4. Sand–fiber admixture after the mixing process performed by four different methods.

$$D_r = \frac{e_{max} - e_r}{e_{max} - e_{min}} \quad (3)$$

where e_{max} and e_{min} are the maximum and minimum void ratios of unreinforced sand, respectively.

The effect of fibers on the properties of the sand was investigated based on random orientations. Hence, to ensure a random distribution of fibers through the entire height of the specimen, all specimens were molded and compacted in one layer.

With the mixing process, the molding processes for lower (0.2% and 0.4%) and higher (1%) percentages of fiber inclusions were different. In the case of 0.2% and 0.4% fiber contents, the admixture was placed into the mold and compacted through vibration as for a pure sand. The 1% fiber-reinforced specimen that was automatically mixed with 10% water content was compacted by tamping, because the vibration method was not appropriate for inputting the entire mass into the determined specimen size for a desired relative density. The specimen preparation was validated by checking the reproducibility of the test results, as illustrated in Fig. 5 (examples of specimens with 60% relative density are given).

2.3. Testing method

Three types of consolidated drained triaxial compression tests were carried out to investigate the effect and contribution of fibers on the mechanical behavior of sand, including the influence on the critical state line:

(1) The effect of relative density on unreinforced and fiber-reinforced sands. Shearing was performed under unique confining pressure on specimen prepared with different initial relative densities (30%, 60% and 80%). Experiments were conducted to investigate the effect of initial relative density (loose, medium dense, and heavily compacted sands) on the mechanical behavior of Toyoura sand with different contents of fiber inclusions (0%, 0.2%, 0.4% and 1%) under the confining pressure of $p' = 100$ kPa.

(2) The effect of confining pressure and fiber content on the mechanical behavior of sand. Shearing was performed under three different confining pressures ($p' = 50$ kPa, 100 kPa and 200 kPa) to compare the effect of the confining pressure on the shear properties for both unreinforced and fiber-reinforced specimens. The range of confining pressures was chosen based on previous studies (Consoli et al., 2009; Diambra et al., 2010; Ibraim et al., 2012). Additional experimentation with a higher confining pressure of 400 kPa was conducted on a 0.2% fiber-reinforced specimen to compare the impact of confining pressure on the stress ratio $\eta\ (= q/p')$ at the end of shearing.

(3) The effect of fiber length on the shear stress parameters. Shearing under 100 kPa confining pressure was performed on 0.2% fiber-reinforced specimens with different fiber lengths. All specimens were prepared with 80% relative density. Experiments were conducted to examine the effect of the fiber length, i.e. aspect ratio, by replacing 12 mm-long fibers with fibers of half ($l_f = 6$ mm) and quarter ($l_f = 3$ mm) lengths. This investigation was performed to check the effect of fiber length on the stress ratio values and the interaction between sand particles and fibers. Furthermore, consideration of the different fiber lengths offers the possibility of achieving calculation of fiber-reinforced sand's void ratio by counting fibers as a part of solids.

After the specimen formation procedure was completed, the saturation process followed. Firstly, CO_2 was infiltrated through the specimen to replace the air in the pores. De-aired water then saturated the specimen, expelling CO_2 as completely as possible. After the saturation process was completed, the degree of saturation was checked using Skempton's B value, which is determined as $B = \Delta u/\Delta\sigma$, where Δu is the increment of pore pressure and $\Delta\sigma$ is the increment of cell pressure under the undrained condition. For all specimens, the B value reached over 0.95.

A complete list of experiments along with the void ratio at the end of consolidation, e_c, and the corresponding relative density D_r, fiber content w_f, fiber length l_f, and confining pressure in the consolidation process p'_0, is given in Table 3. Experimental results of reference tests are given with indices a and b. The confining pressure can be obtained by back pressure of 200 kPa and cell pressures of 250 kPa, 300 kPa, 400 kPa and 600 kPa. The tests were carried out according to the Japanese standard JGS 0524–2020 (2020) with a strain rate of 0.5% per minute until the axial strain reached 20% (capacity of the triaxial apparatus). Loading was applied from the upper part of the specimen by the air pressure supplied to the bellofram cylinder with an internal load cell (gage based transducer) of 5 kN capacity. The axial strain was measured using a linear variable differential transformer (LVDT) placed outside the triaxial cell. The displacement that controls the supplied pressure to the bellofram cylinder and applies load at a constant strain rate was monitored. Volumetric strain was measured by a strain gage based transducer connected to the drainage burette.

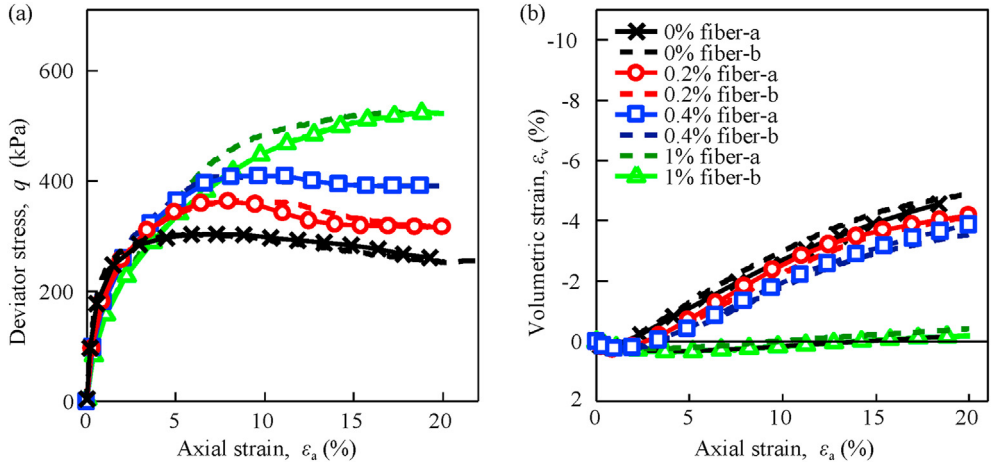

Fig. 5. Reference tests to confirm reproducibility of the experiments ($D_r = 60\%$ and $p'_0 = 100$ kPa).

Table 3
List of experiments.

Test	w_f (%)	l_f (mm)	e	D_r (%)	p'_0 (kPa)	$\eta_r = q_r/p'$
L100-00	0	–	0.823	30	100	1.34
M100-00-a	0	–	0.771	60	100	1.34
M100-00-b	0	–	0.772	60	100	1.34
D-050-00	0	–	0.721	80	50	1.34
D-100-00	0	–	0.719	80	100	1.34
D-200-00	0	–	0.717	80	200	1.34
D-100-02	0.2	3	0.717	80	100	1.43
D-100-02	0.2	6	0.718	80	100	1.48
L100-02	0.2	12	0.829	30	100	1.52
M100-02-a	0.2	12	0.77	60	100	1.52
M100-02-b	0.2	12	0.773	60	100	1.52
D-050-02	0.2	12	0.715	80	50	1.52
D-100-02	0.2	12	0.713	80	100	1.53
D-200-02	0.2	12	0.709	80	200	1.52
D-400-02	0.2	12	0.699	80	400	1.52
L100-04	0.4	12	0.821	30	100	1.71
M100-04-a	0.4	12	0.772	60	100	1.71
M100-04-b	0.4	12	0.774	60	100	1.71
D-050-04	0.4	12	0.712	80	50	1.72
D-100-04	0.4	12	0.712	80	100	1.71
D-200-04	0.4	12	0.705	80	200	1.71
M100-10-a	1	12	0.775	60	100	1.87
M100-10-b	1	12	0.772	60	100	1.87
D-050-10	1	12	0.711	80	50	1.88
D-100-10	1	12	0.708	80	100	1.85
D-200-10	1	12	0.705	80	200	1.81

Note: L – Loose; M – Medium dense; D – Dense.

3. Test results and discussion

3.1. Stress and strain notations

Conventional stress and strain variables were used for axisymmetric triaxial conditions. The deviatoric stress q and the mean effective stress p' were the stress invariants, and the volumetric strain ε_v and axial strain ε_a were the strain invariants. These invariants are defined under the triaxial shear condition:

$$p' = \frac{1}{3}(\sigma'_1 + 2\sigma'_3),\ q = \sigma'_1 - \sigma'_3,\ \varepsilon_a = \frac{2}{3}(\varepsilon_1 - \varepsilon_3),\ \varepsilon_v = \varepsilon_1 + 2\varepsilon_3 \quad (5)$$

where σ'_1 and σ'_3 indicate the maximum and minimum effective principal stresses, respectively; and ε_1 and ε_3 are the maximum and minimum principal strains, respectively. Volumetric change was investigated according to the specific volume $v = 1 + e$.

3.2. The effect of relative density on unreinforced and fiber-reinforced sands

The results of the drained triaxial compression tests under 100 kPa confining pressure, performed on both unreinforced and reinforced sands prepared with different initial relative densities are given in Figs. 6–9, including deviatoric stress–axial strain (q-ε_a), deviatoric stress–mean effective stress (q-p'), specific volume–axial strain (v-ε_a), and specific volume–mean effective stress (v-p') curves.

Fig. 6 shows the typical stress–strain and volumetric change behaviors of unreinforced sand with 30%, 60% and 80% initial relative densities.

It is convenient, first, to consider the effect of relative density on sands sheared under unique confining pressure through the existing common framework. Loose specimens in a drained triaxial compression test typically exhibit only strain-hardening behavior without a marked peak in the stress–strain relationship and reach the flat maximum at the end of the shearing. Loose specimens compress and the volumetric strain increases as the shearing proceeds. On the other hand, dense specimens exhibit strain-hardening behavior, reaching a marked peak which turns into strain-softening behavior with decrease of deviatoric stress towards the ultimate point. Dense specimens contract slightly at lower levels of strain, which is followed by strong expansion until the end of the test.

Similarly, Toyoura sand specimens with 80% and 60% relative densities showed strain-hardening behavior until a marked peak deviatoric stress was reached, which was followed by strain-softening until ultimate residual stresses. Dense specimens showed slight contraction at very low strain levels, which was followed by strong expansion until the end of the test. Specimens with 80% and 60% relative densities were regarded as dense and medium dense sands, respectively. In contrast, the specimen of Toyoura sand with 30% relative density experienced only strain-hardening behavior and reached a flat maximum at about 20% axial strain. The loose specimen initially showed higher compression and began expanding slightly at higher strains until the end of the shearing. Specimens with 30% relative density were regarded as medium loose.

Fig. 7 shows the drained compression test results performed on 0.2% fiber-reinforced specimens with initial relative densities of 30%, 60% and 80%. The sand specimens with 0.2% fiber content showed similar mechanical behavior with unreinforced sand. The loose specimen with $D_r = 30\%$ in q-ε_a curve experienced only hardening behavior while reaching a flat maximum deviatoric stress q_{max} at 20% axial strain. In volumetric change curves (v-ε_a and v-p'), the loose specimen initially compressed up to 5% axial strain, which was then followed by expansion towards the maximum value of specific volume. In contrast, the denser specimens exhibited a marked peak in q-ε_a curve, and deviatoric stress decreased with the shear progression, i.e. denser specimens underwent both hardening and softening behaviors.

In v-ε_a and v-p' curves, denser specimens showed smaller initial contraction, and then expanded considerably up to the end of shearing. Although each q-ε_a curve was different and q_{max} increased

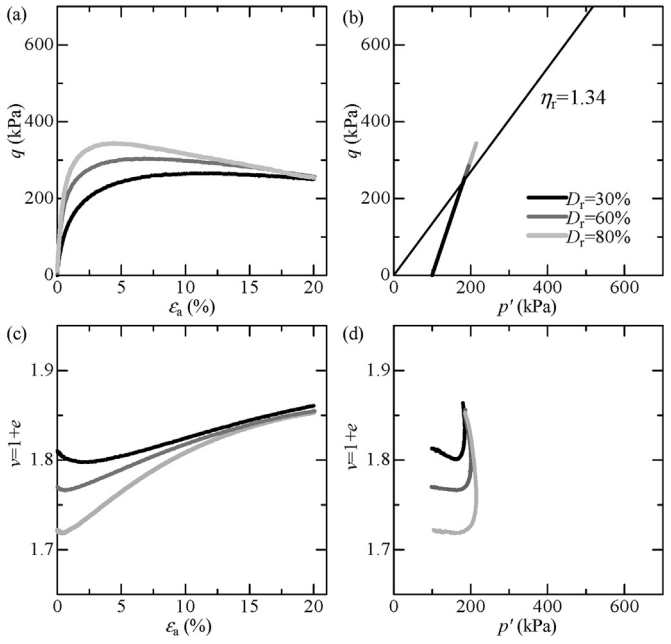

Fig. 6. Shear–strain–volumetric response of unreinforced sand for 100 kPa confining pressure prepared with different initial relative densities.

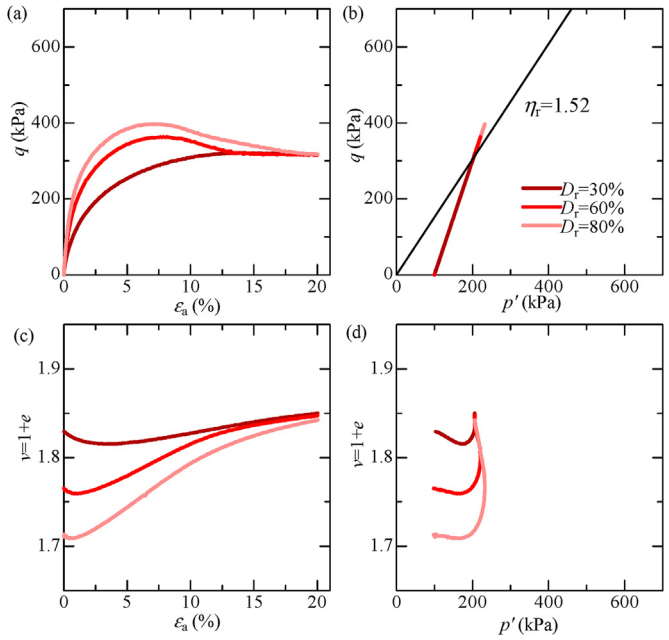

Fig. 7. Shear–strain–volumetric response of 0.2% fiber-reinforced sand for 100 kPa confining pressure prepared with different initial relative densities.

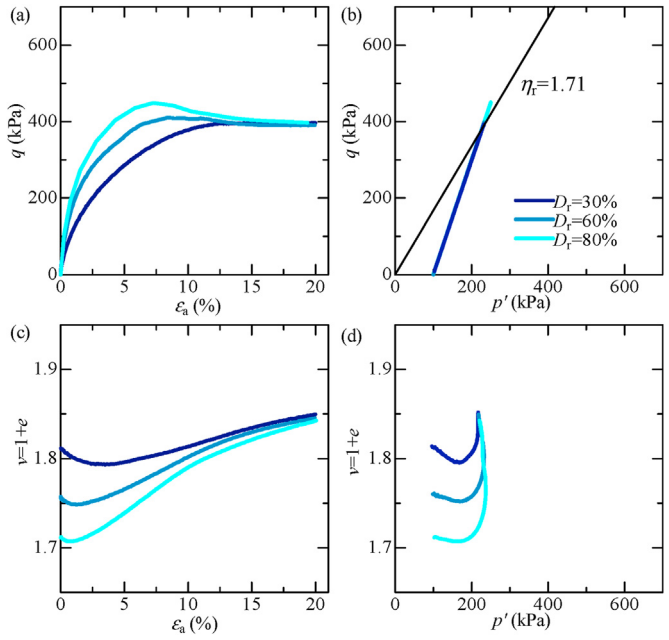

Fig. 8. Shear–strain–volumetric response of 0.4% fiber-reinforced sand for 100 kPa confining pressure prepared with different initial relative densities.

with initial relative density, the residual stresses q_r for all fiber-reinforced specimens with fiber content of 0.2% were almost the same and equaled approximately to 315 kPa, independent of the initial relative density (Fig. 7a). All specific volumes v and the mean effective stresses p' also tended to reach the same values at the end of shearing despite initial differences in specific volumes, as shown in Fig. 7b–d. Moreover, the volumetric change behavior in v-ε_a curves experienced less expansion with $v = 1.85$ than the unreinforced specimen at 20% axial strain (Fig. 7c and d).

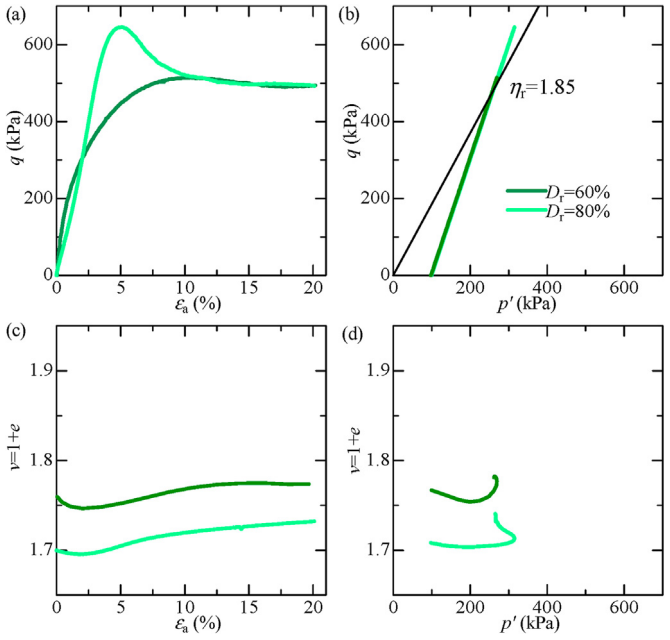

Fig. 9. Shear–strain–volumetric response of 1% fiber-reinforced sand for 100 kPa confining pressure prepared with different initial relative densities.

Fig. 8 represents the results from drained triaxial compression performed on sandy specimens with 0.4% fiber content and different initial relative densities. The mechanical behavior of 0.4% fiber-reinforced sand had the same tendency as the unreinforced and reinforced sands with 0.2% fiber content and underwent similar shear behavior. Explicitly, the fiber-reinforced specimens exhibited higher maximum and residual deviatoric stresses than the unreinforced specimen for all relative densities. The residual stresses q_r, mean effective stresses p' and specific volumes v tended to reach the same value at the end of shearing despite the difference in the initial relative density, i.e. $q_r = 380$ kPa, $p' = 210$ kPa and $v = 1.84$ at an axial strain of 20%. Compared to the 0% and 0.2% fiber contents, 0.4% fiber-reinforced specimens had more pronounced maximum deviatoric stress and sharper passage to the residual state.

Particularly, unreinforced Toyoura sand specimens exhibited different q-ε_a curves depending on the initial relative densities, whereas the deviatoric stresses tended to reach the same residual stresses $q_r = 250$ kPa at 20% axial strain. This behavior could also be observed in v-ε_a and v-p' curves, where all specimens tended to reach the same value of specific volume of 1.86 after shearing, despite the difference in the initial relative densities. It should be noted that the volumetric change still exists, but with a very small increment. Also, despite small changes, all three specific volumes have the same mean effective stress values of $p' = 180$ kPa at the end of shearing. Regardless of the initial void ratio, the stresses and volumes converged to a common value at the end of the tests. This is a property that is commonly found in the critical state of soils (Schofield and Wroth, 1968; Atkinson and Bransby, 1978), where the existence of the critical state of sand was presented. Therefore, it is assumed that the Toyoura sand at the end of the tests has reached the vicinity of the critical state as in the previous studies.

The drained shear behavior of 0.2% and 0.4% fiber-reinforced sand quite resembles those of unreinforced sand. Overall, the effect of different relative densities on the shear-strain-volumetric response of unreinforced Toyoura sand was also observed in the case of fiber-reinforced Toyoura sand. Since the stress and volume changes converged to a certain value in both cases as in the

unreinforced case, despite a very small increment in the specific volumes, it can be considered that the fiber-reinforced sand had also reached the vicinity of the critical state at the end of the tests.

Compared with the lower percentage of reinforcing material, 1% fiber-reinforced specimens exhibited some differences in their mechanical behavior (Fig. 9). The maximum and residual deviatoric stresses were higher, while volumetric expansion was significantly low. In v-ε_a and v-p' curves, the specific volumes of 60% and 80% relative densities did not reach the same value at the end of shearing. That may be because of the difficulties in specimen preparation compared with specimens having lower percentages of fiber inclusions of 0.2% and 0.4%. Because of the difference in the molding process, the result of 1% fiber-reinforced sand prepared in a loose condition (D_r = 30%), where molding did not require tamping, was not included in direct comparison with denser specimens molded through tamping. Further investigation is needed to understand the behavior of 1% fiber-reinforced specimens, which have a higher percentage of fiber inclusions.

Fig. 10 shows the detailed volumetric change behavior by comparison of the shear behavior of unreinforced and 0.4% fiber-reinforced sands. From v-ε_a curve around the initial stage of shearing, the amount of compression of sand mixed with fibers was larger than that of unreinforced sand, and the axial strain from compression to expansion was up to 3% (blue arrow), which was also slightly larger than that of the unreinforced sand (black arrow), about 1%. Focusing on the behavior around the maximum deviatoric stress in v-p' curves, sand with fibers had larger v and p' at maximum deviatoric stress (point B_1) than unreinforced sand (A_1). Even though the specific volume of reinforced sand was higher (point B_1, v-p' curves) than that of unreinforced sand (point A_1, v-p' curves), the sand with fibers exhibited larger mean effective stress than the unreinforced sand, and thus larger maximum deviatoric stress (points A_1 and B_1 on the q-p' curves, respectively). The fiber insertion effect is shown as the increase of the amount of compression at the initial stage of shearing and the axial strain from compression to expansion; and even though the expansion due to the shearing is allowed and the specific volume becomes high at around the maximum deviatoric stress, the residual stress increases with the increase of the confining pressure. Therefore, the sand mixed with fibers showed higher peak and post-peak deviatoric stresses (shear strength) than the unreinforced sand, while experiencing less volumetric expansion.

Despite using PVA fibers with a higher Young's modulus and tensile strength than previous studies (Yetimoglu and Salbas, 2003; Diambra et al., 2010; Ibraim et al., 2012) where polypropylene fibers were used, the initial stiffness decreased with the increase in fiber content (Fig. 10). The deformation modulus $E_{50} = 0.5q_{max}/\varepsilon_{50}$ was used to express the initial stiffness of both unreinforced and reinforced sands, where ε_{50} is the axial strain at half of the maximum deviatoric stress (Fig. 11). The initial stiffness of the fiber-reinforced sand was lower than that of unreinforced sand under all relative densities. Similar outcomes were presented in previous studies (Michalowski and Čermak, 2003; Heineck et al., 2005). The initial stiffness eventually decreased with the increase in fiber content. Because of the difference in specimen preparation methods between lower and higher fiber inclusions, the results cannot be directly compared. Therefore, the results were illustrated by different types of lines representing different specimen preparation methods.

To compare the trend and effect of fibers on the stress ratio, Fig. 12 plots the stress ratio η ($= q/p'$)—axial strain ε_a dependency. It shows that the adding of fibers increases the stress ratio relative to the fiber content increment. Furthermore, the stress ratios of unreinforced and fiber-reinforced sand specimens reached the same values for a definite fiber contents at the end of shearing, independent of the initial relative density.

Fig. 13 represents phase transformation stress ratio η_{pt} ($= q_{pt}/p'$) (change from elastic compression to plastic expansion), peak stress ratio η_{max} ($= q_{max}/p'$), and residual stress ratio η_r ($= q_r/p'$) dependency on relative densities. It should be noted that the stress ratio values at phase transformation point and maximum shear strength increase with the increase in relative density (Fig. 13a and b). From Fig. 13c, it can be confirmed that the unreinforced sand and sand reinforced with 0.2% and 0.4% fiber contents have stress ratio η_r ($= q_r/p'$) values of 1.34, 1.52 and 1.71, respectively, at 20% axial strain. In case of 1% fiber-reinforced sand, despite reaching the same value of stress ratio, a similar conclusion cannot be made in the same way as for a lower percentage of fiber inclusions. The issue concludes in a perceptible difference in mechanical behavior, especially in volumetric change characteristics.

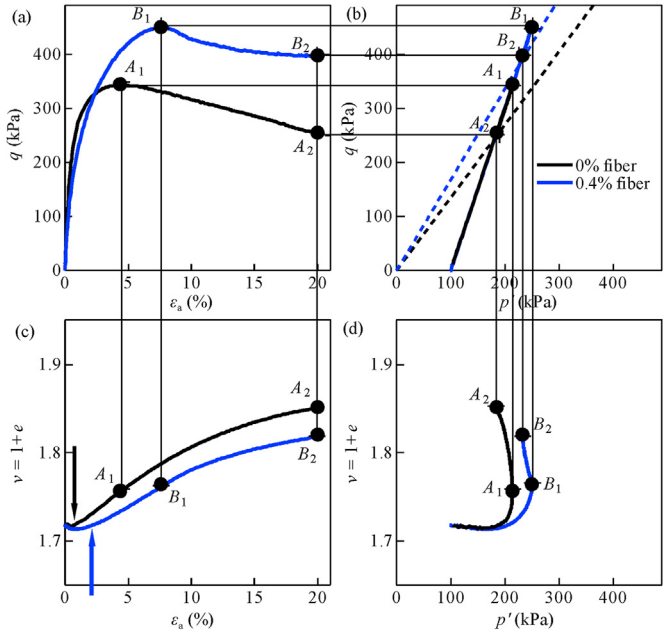

Fig. 10. Shear strength and volumetric change behaviors of unreinforced and 0.4% fiber-reinforced sands.

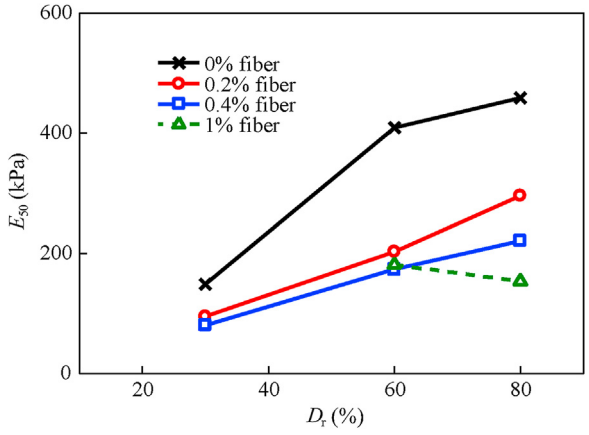

Fig. 11. Initial stiffness–relative density dependency, expressed through the deformation modulus E_{50} (solid lines – dry vibration, dashed line – moist tamping).

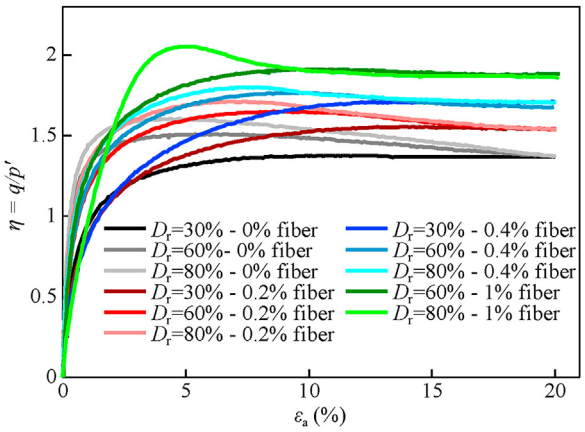

Fig. 12. Stress ratio–axial strain dependency for all fiber contents with different initial relative densities.

3.3. The effects of confining pressure and fiber content on the mechanical behavior of sand

Convinced of the existence of a critical state for fiber-reinforced sand as in the case of unreinforced sand, an additional series of experiments was performed to compare the effect of the confining pressure on the shear properties of unreinforced and fiber-reinforced specimens. Figs. 14–17 represent the shear behaviors of unreinforced and reinforced sands with 0.2%, 0.4% and 1% fiber contents, respectively, under different confining pressures.

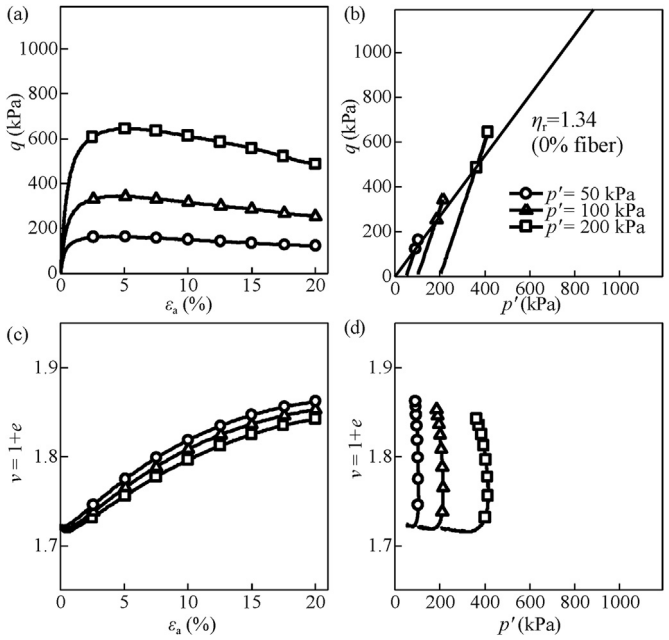

Fig. 14. Shear–strain–volumetric response of unreinforced sand for 50 kPa, 100 kPa, and 200 kPa confining pressures prepared with D_r = 80%.

Fig. 14 shows the typical shear characteristics of densely packed sand with both hardening and softening behaviors. Higher confining pressure produces higher shear stress with the increase in the shear modulus, peak and residual stresses. Additionally, when the relatively high confining pressure is applied to a dense

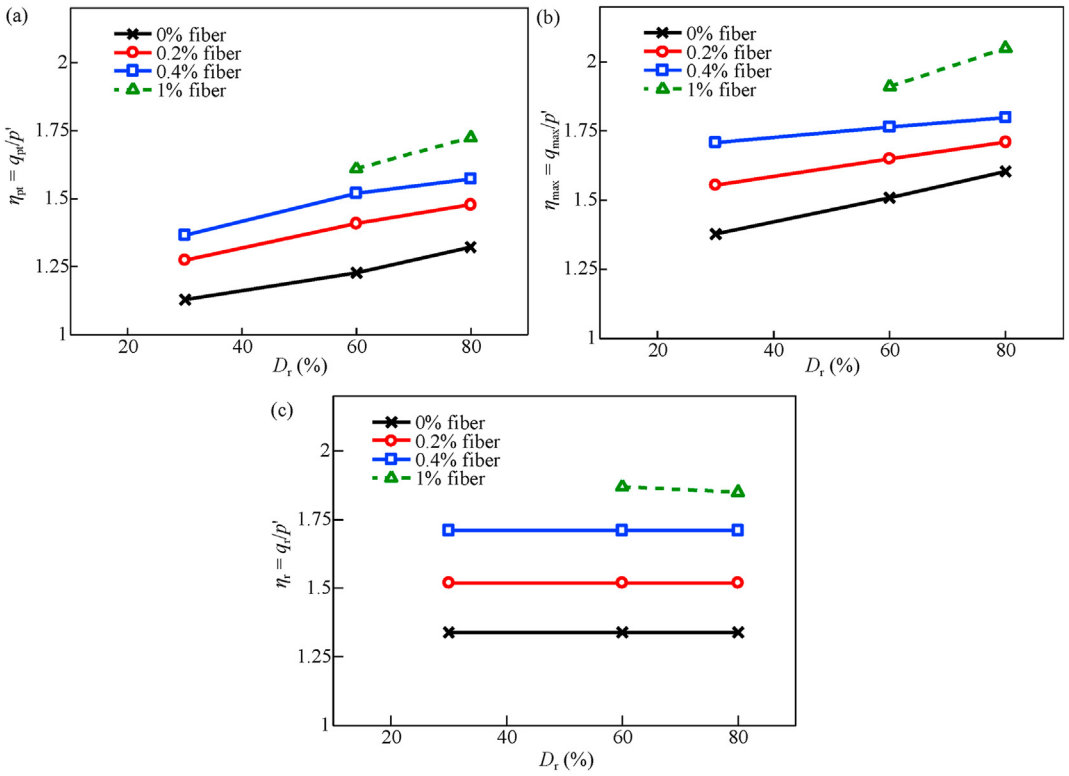

Fig. 13. Stress ratio dependency on relative density: (a) Phase transformation, (b) peak, and (c) residual stress ratios (solid lines – dry vibration, dashed line – moist tamping).

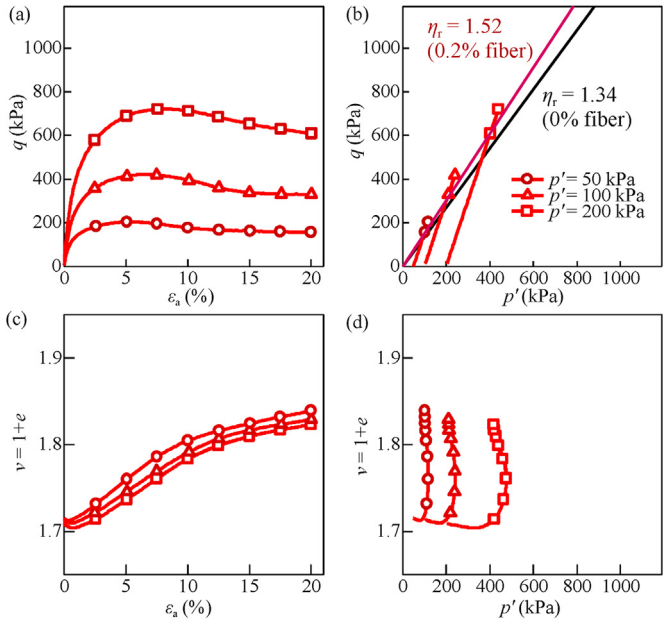

Fig. 15. Shear–strain–volumetric response of 0.2% fiber-reinforced sand for 50 kPa, 100 kPa and 200 kPa confining pressures prepared with D_r = 80%.

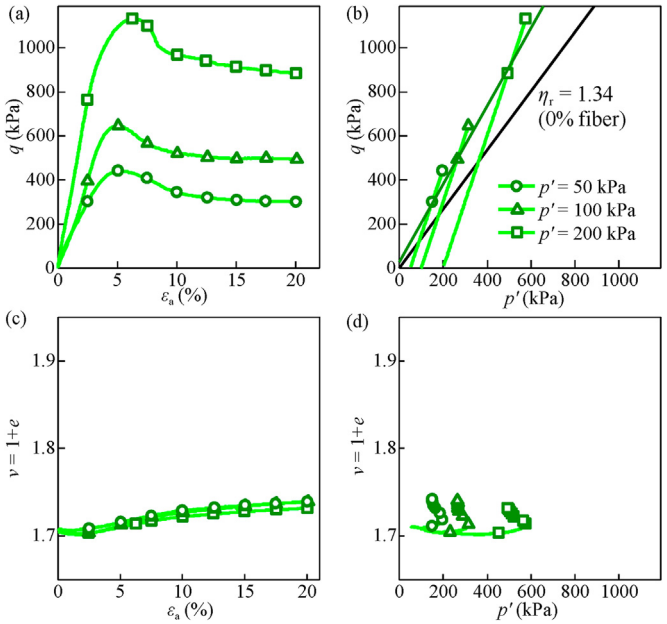

Fig. 17. Shear–strain–volumetric response of 1% fiber-reinforced sand for 50 kPa, 100 kPa and 200 kPa confining pressures prepared with D_r = 80%.

specimen, the shear-strain-volumetric response is quite similar to the behavior of a looser specimen, i.e. less marked peak stress and less volumetric expansion. Toyoura sand specimens sheared under different confining pressures showed identical behavior. Higher confining pressure increased maximum and residual deviatoric stresses and decreased volumetric expansion, i.e. greater confining pressure, and less volumetric expansion that can be confirmed on both v-ε_a and v-p' curves. Connection of all three values of the stress ratios η at 20% axial strain in q-p' curve is a straight line through the origin of the stress plane (Fig. 14b). Also, despite the difference in stress paths, the values of residual stress ratio were equal to η_r = 1.34 for all confining pressures, which was the same as the value in the case of different initial relative densities (Section 3.2). Therefore, as mentioned in previous studies (Schofield and Wroth, 1968; Atkinson and Bransby, 1978), pure sand can be idealized as having the critical state line.

Fiber-reinforced sand specimens experienced identical mechanical behavior to the unreinforced one: the maximum and residual stresses increased, and the volumetric expansion at 20% axial strain decreased with the increase in confining pressure. The effect of fiber inclusions was represented by a higher and more pronounced maximum deviatoric stress q_{max} and higher residual deviatoric stress q_r compared to sand specimens without fibers, which can be observed in q-ε_a curves (Figs. 15a, 16a and 17a). As shown in Figs. 15b and 16b, the stress states at the end of shearing were on a straight line through the origin in q-p' plane. The tendency was similar to that of unreinforced sand. By idealizing the existence of a critical state (Section 3.2), it can be considered that the critical state line existed in the fiber-reinforced sand depending on the fiber content, as well as in the unreinforced sand. The same

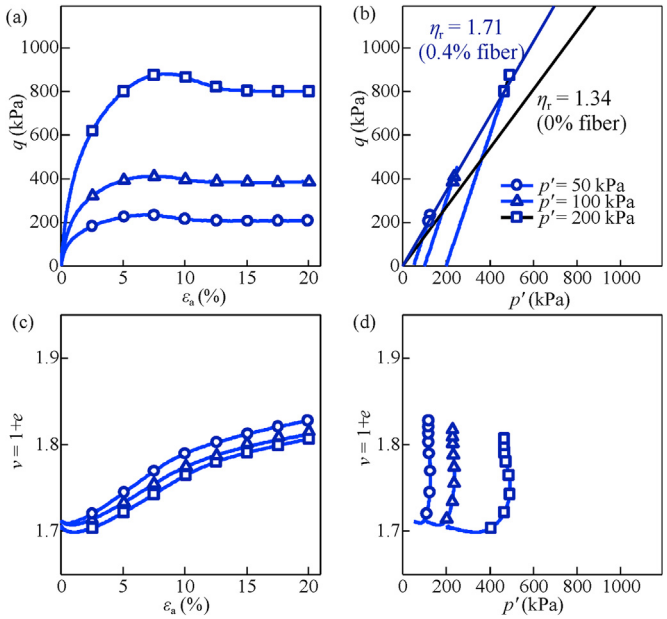

Fig. 16. Shear–strain–volumetric response of 0.4% fiber-reinforced sand for 50 kPa, 100 kPa and 200 kPa confining pressures prepared with D_r = 80%.

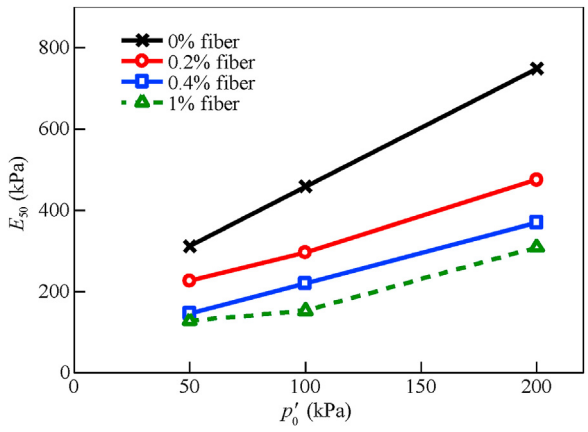

Fig. 18. Initial stiffness–confining pressure dependency, expressed by the deformation modulus E_{50} (solid lines – dry vibration, dashed line – moist tamping).

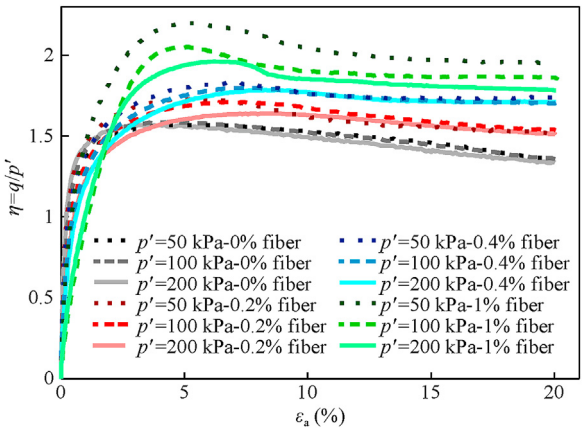

Fig. 19. Stress ratio–axial strain dependency for all fiber contents of sand sheared under 50 kPa, 100 kPa and 200 kPa confining pressures.

conclusion cannot be drawn for 1% fiber-reinforced sand (Fig. 17b), where the stress states at 20% axial strain were on a straight line, but not through the origin in q-p' plane.

Initial stiffness of fiber-reinforced sand was smaller than that of pure sand under all three confining pressures considered (Fig. 18). Furthermore, initial stiffness of both unreinforced and fiber-reinforced sands increased with the increase in confining pressure.

In order to consider the effects of fiber content and confining pressure on the stress ratio, the stress ratio η $(= q/p')$ is plotted against the axial strain ε_a in Fig. 19. The trend of stress ratio increasing with the fiber content is obvious for all fiber contents and confining pressures. The respective residual stress ratio values η_r $(= q_r/p')$ of 0%, 0.2% and 0.4% fiber inclusions reached the same value at 20% axial strain, independent of the confining pressure, even though η values at lower axial strain values were different for each confining pressure.

A detailed description of the stress ratios at phase transformation point, maximum shear stress and residual stress is given in Fig. 20. The phase transformation and peak stress ratios of fiber-reinforced sand were higher than those of unreinforced sand; stress ratio values increased with the increase in fiber content. It should be noted that the increase in confining pressure led to a slight decrease in phase transformation and peak stress ratios of both unreinforced and fiber-reinforced sand. However, the residual stress ratios η_r $(= q_r/p')$ at 20% axial strain is the same respective values with 1.34 for unreinforced sand, whereas those for reinforced sand with 0.2% and 0.4% of fiber contents are equal to 1.52 and 1.71, respectively (Fig. 20c). Nevertheless, compared to a lower percentage of fiber inclusions, 1% fiber-reinforced sand experienced a significantly different trend for a residual stress ratio with the increase in confining pressures, that is, with the increase in confining pressure, the residual stress ratio η_r decreased.

Volumetric change responses of fiber-reinforced sands are presented through the specific volume dependency from an axial strain and mean effective stress in Fig. 15c and d, 16c and d, and 17c and d. The initial volumetric compression increased and the final volumetric expansion decreased with the increase in fiber content. The specific volume of sand with 0.2% and 0.4% fiber contents decreased as the confining pressure increased at the end of shearing. It can also be observed in Fig. 21, where the lines that connect values of specific volumes at 20% axial strain, depending on the initial confining pressures, are compared to the volumetric change of unreinforced sand. The lines are almost parallel, and decline with the fiber content.

Additional experimentation with higher confining pressure $(p'_0 = 400$ kPa) was performed on 0.2% fiber-reinforced sand. As can

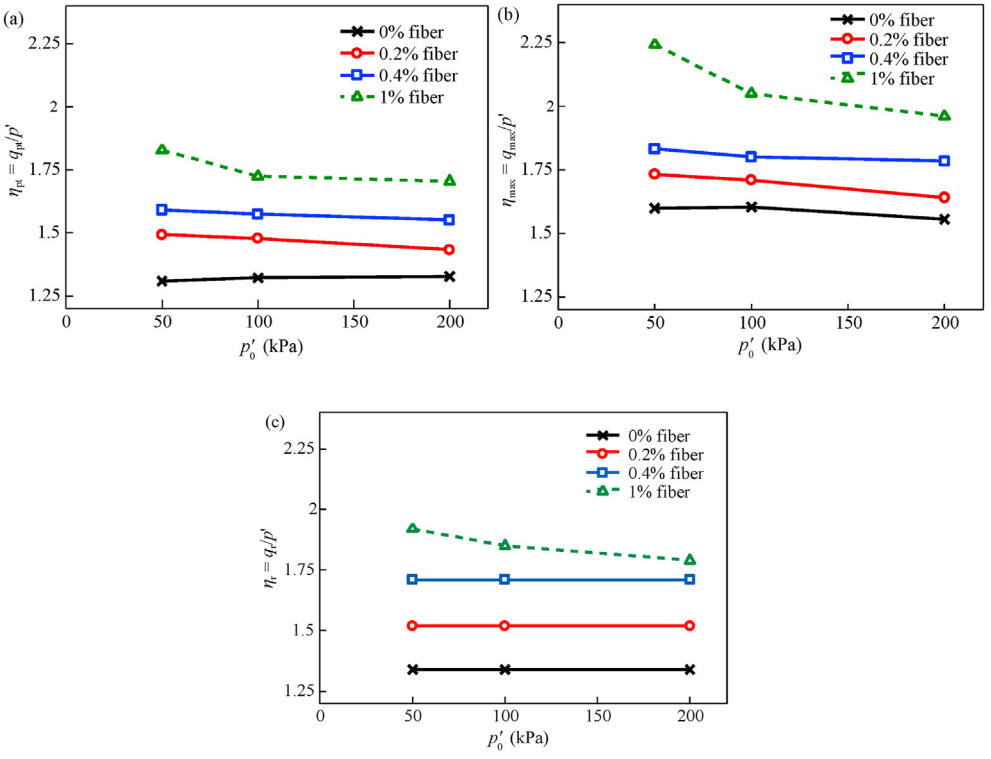

Fig. 20. Stress ratio dependency on confining pressure: (a) Phase transformation; (b) Peak stress ratio; and (c) residual stress ratio (solid lines – dry vibration, dashed line – moist tamping).

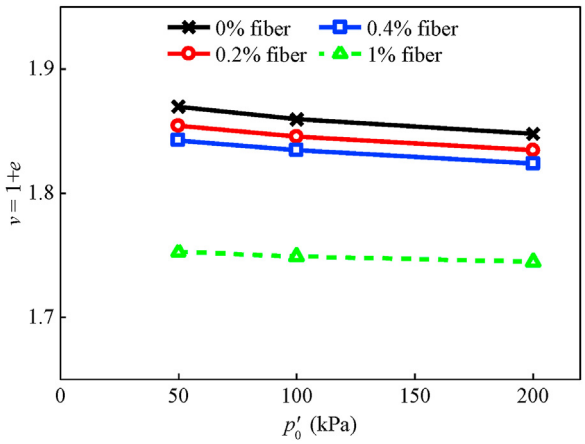

Fig. 21. Specific volume v at 20% axial strain–confining pressure p'_0 dependency with the fiber content (solid lines – dry vibration, dashed line – moist tamping).

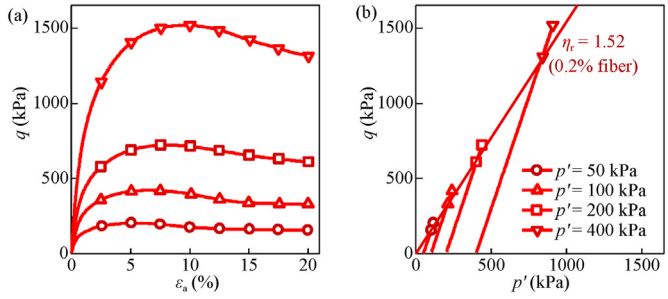

Fig. 22. Stress–strain response of 0.2% fiber-reinforced sand for 50 kPa, 100 kPa, 200 kPa and 400 kPa confining pressures.

be seen from Fig. 22, contribution of fibers increased the deviatoric stress with the increase in confining pressure, while the stress ratio at the end of shearing was on the critical state line obtained from the shear results under lower confining pressures. This means that once the fiber content was determined, the critical state line corresponding to the fiber content was also determined.

3.4. The effect of fiber length on the shear stress parameters

Fig. 23 presents the shear behavior of unreinforced and 0.2% fiber-reinforced sands with different fiber lengths (12 mm, 6 mm and 3 mm, respectively). The aspect ratios of 12 mm-, 6 mm-, and 3 mm-long fibers were 300, 150, and 75, respectively. The specimens were prepared in dense condition with the initial relative density of 80% and sheared under 100 kPa confining pressure. Sand reinforced with 3 mm- and 6 mm-long fibers experienced slightly higher maximum and residual deviatoric stresses in q-ε_a curves, with lower volumetric expansion than unreinforced sand. The effect of the fiber length can be concluded as follows: the longer fibers have higher maximum and residual deviatoric stresses with lower volumetric expansion. Furthermore, shortening the fiber length leads to decrease in deviatoric and mean effective stresses and increase in volumetric expansion, i.e. it approaches the shear–strain–volumetric change behavior of unreinforced sand. These observed results are consistent with those of previous studies, where the effect of fibers on the shear strength was considered (Gray and Ohashi, 1983; Consoli et al., 2009; Sadek et al., 2010; Falorca and Pinto, 2011; Lirer et al., 2011). Moreover, according to

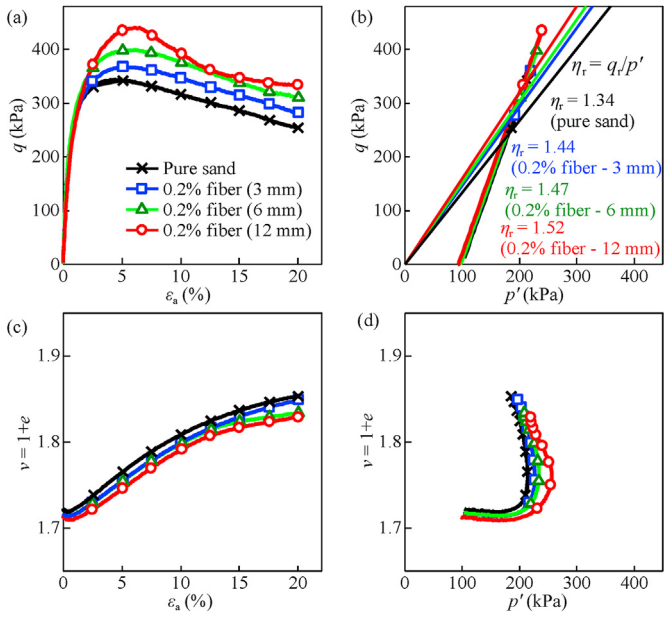

Fig. 23. Stress–strain–volumetric change behavior of unreinforced sand and sand reinforced with 0.2% fiber content of different lengths.

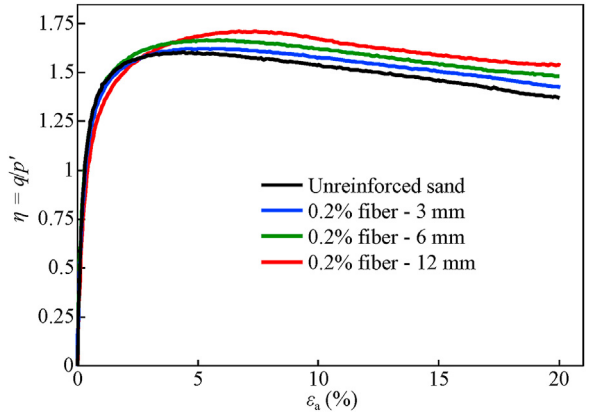

Fig. 24. Influence of fiber length on the stress ratio (critical state line parameter).

Michalowski and Ĉermak (2003), the reinforcement is effective when the length of reinforcing material is one order higher than the host soil.

As decreasing the length of fiber leads to decreases in maximum and residual deviatoric stresses, and mean effective stress, the determination of the void ratio of fiber-reinforced sand should be done by considering the fibers as a part of solids. In the case that the fibers are counted as a part of voids, such variation of the shear behavior would not be observed, i.e. there would be no apparent effect of the fiber length.

Fig. 24 represents the stress ratio η–axial strain ε_a dependency. As can be observed, with the decrease in the length of reinforcing material, the residual stress ratio values decrease ($\eta_r = 1.52$% for 0.2% fiber with 12 mm length, $\eta_r = 1.48$ for 0.2% fiber with 6 mm length, $\eta_r = 1.43$ for 0.2% fiber with 3 mm length, and $\eta_r = 1.34$ for 0% fiber). The influence of fiber length on the stress ratio is given in Fig. 25.

4. Conclusions

The effect of short discrete PVA fibers on the drained shear behavior of Toyoura sand was examined through consolidated

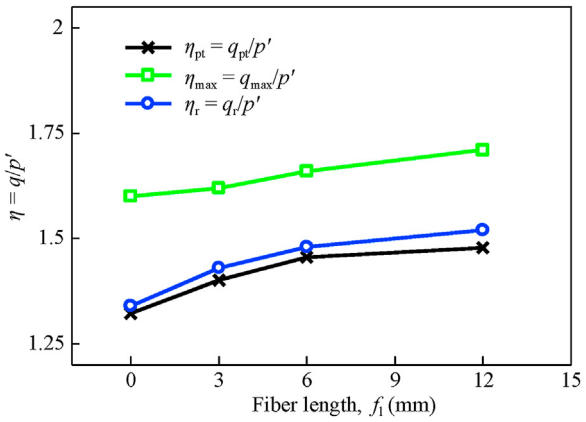

Fig. 25. Stress ratio dependency on fiber length with 0.2% fiber inclusions (legends show different stress ratios).

drained triaxial compression tests. The main conclusions are drawn as follows:

(1) A more suitable specimen preparation method was obtained by checking the mechanical behavior of specimens with high reproducibility of test results from four methods. In case of lower percentage of fiber inclusions (0.2% and 0.4%), the method was to mix the fibers manually with dry sand and to mold the mixture through vibration.

(2) The drained shear behavior of fiber-reinforced sand with 0.2% and 0.4% fiber contents under the same confining pressure with different initial relative densities exhibited similar behavior to unreinforced sand. At the end of shearing (20% axial strain), the respective deviatoric stresses were approximately the same, and the specific volume reached almost the same value even if the initial relative density was different. Hence, according to this observed mechanical behavior, it is considered that the stress state at the end of shearing is near critical state.

(3) The shear behavior of fiber-reinforced sand under different confining pressures exhibited similar behavior to unreinforced sand. The test results of changing the confining pressure indicate that the critical state line exists in the fiber-reinforced sand as well as in unreinforced sand. It is a straight line through the origin in q-p' plane and the slope of the critical state line increased as the fiber content increased. In v-p' space, the specific volume decreased as the confining pressure increased. Furthermore, the shorter the fiber, the smaller the slope of the critical state line in q-p' plane, which approaches that of pure sand.

Based on the observed shear characteristics and consistent outcomes of stress ratio values (critical state line), the mechanical behavior of fiber-reinforced sand as well as pure sand will be considered through the critical state concept. Further investigation on the effect of fiber on the shear characteristics of sand will be performed, and mechanical behavior will be expressed by a constitutive model, by estimating the critical state parameters obtained in this study.

Declaration of competing interest

The authors declare that they have no known competing financial interests or personal relationships that could have appeared to influence the work reported in this paper.

References

Ajayi, O., Le Pen, L., Zervos, A., Powrie, W., 2017. Scaling relationships for strip fibre-reinforced aggregates. Can. Geotech. J. 54 (5), 710–719.

Atkinson, J.H., Bransby, P.L., 1978. The Mechanics of Soils: an Introduction to Critical State Soil Mechanics. McGraw-Hill, London, UK.

Chen, C., 2010. Triaxial compression and extension for fiber-reinforced silty sand. In: Puppala, A.J., Huang, J., Han, J., Hoyos, L.R. (Eds.), Ground Improvement and Geosynthetics: Proceedings of Sessions GeoShanghai 2010. American Society of Civil Engineers (ASCE), Reston, VA, USA, pp. 367–376.

Consoli, N.C., Casagrande, M.D.T., Coop, M.R., 2007b. Performance of fiber-reinforced sand at large shear strains. Geotechnique 57 (9), 751–756.

Consoli, N.C., Festugato, L., Heineck, K.S., 2009. Strain-hardening behaviour of fibre-reinforced sand in view of filament geometry. Geosynth. Int. 16 (2), 109–115.

Consoli, N.C., Heineck, K.S., Casagrande, M.D.T., Coop, M.R., 2007a. Shear strength behavior of fiber-reinforced sand considering triaxial tests under distinct stress path. J. Geotech. Geoenviron. Eng. 133 (11), 1466–1469.

Diambra, A., Ibraim, E., Muir Wood, D., Russell, A.R., 2010. Fibre reinforced sands: experiments and modelling. Geotext. Geomembranes 28 (3), 238–250.

Eldesouky, H.M., Morsy, M.M., Mansour, M.F., 2016. Fiber-reinforced sand strength and dilation characteristics. Ain Shams Eng. J. 7 (2), 517–526.

Falorca, I.M.C.F.G., Pinto, M.I.M., 2011. Effect of short, randomly distributed polypropylene microfibers on shear strength behaviour of soils. Geosynth. Int. 18 (1), 2–11.

Gao, Z., Huang, M., 2021. Effect of sample preparation on mechanical behavior of fibre-reinforced sand. Comput. Geotech. 133, 104007.

Gray, D.H., Ohashi, H., 1983. Mechanics of fiber reinforcement in sands. J. Geotech. Eng. 109 (3), 335–353.

Heineck, K.S., Coop, M.R., Consoli, N.C., 2005. Effect of microreinforcement of soils from very small to large shear strains. J. Geotech. Geoenviron. Eng. 131 (8), 1024–1033.

Ibraim, E., Diambra, A., Russell, A.R., Muir Wood, D., 2012. Assessment of laboratory sample preparation for fibre reinforced sands. Geotext. Geomembranes 34, 69–79.

Ibraim, E., Fourmont, S., 2006. Behaviour of sand reinforced with fibres. In: Ling, H.I., Callisto, L., Leshchinsky, D., Koseki, J. (Eds.), Soil Stress-Strain Behavior: Measurement, Modeling and Analysis. Solid Mechanics and its Applications, vol. 146. Springer, Dordrecht, Netherlands, pp. 807–918.

Jewell, R.A., Wroth, C.P., 1987. Direct shear tests on reinforced sand. Geotechnique 37 (1), 53–68.

JGS 0131–2015, 2015. Test Method for Particle Size Distribution of Soils. Japanese Geotechnical Society, Tokyo, Japan.

JGS 0524–2020, 2020. Method for Consolidated-Drained Triaxial Compression Test on Soils. Japanese Geotechnical Society, Tokyo, Japan.

Lirer, S., Flora, A., Consoli, N.C., 2011. On the strength of fibre-reinforced soils. Soils Found. 51 (4), 601–609.

Liu, J., Wang, G., Kamai, T., Zhang, F., Yang, J., Shi, B., 2011. Static liquefaction behavior of saturated fiber-reinforced sand in undrained ring-shear tests. Geotext. Geomembranes 29 (5), 462–471.

Maher, M.H., Gray, D.H., 1990. Static response of sands reinforced with randomly distributed fibers. J. Geotech. Eng. 116 (11), 1661–1677.

Michalowski, R.L., Čermak, J., 2003. Triaxial compression of sand reinforced with fibers. J. Geotech. Geoenviron. Eng. 129 (2), 125–136.

Muir Wood, D., Diambra, A., Ibraim, E., 2016. Fibres and soils: a route towards modelling of root-soil systems. Soils Found. 56 (5), 765–778.

Roscoe, K.H., Burland, J.B., 1968. On the generalized stress-strain behavior of 'wet' clay. In: Heyman, J., Leckie, F.A. (Eds.), Engineering Plasticity. Cambridge University Press, Cambridge, UK, pp. 535–609.

Roscoe, K.H., Schofield, A.N., Wroth, C.P., 1958. On the yielding of soils. Geotechnique 8 (1), 22–53.

Sadek, S., Najjar, S.S., Freiha, F., 2010. Shear strength of fiber-reinforced sands. J. Geotech. Geoenviron. Eng. 136 (3), 490–499.

Schofield, A.N., Wroth, C.P., 1968. Critical State Soil Mechanics. McGraw-Hill, Cambridge, UK.

Silva Dos Santos, A.P.S., Consoli, N.C., Baudet, B.A., 2010. The mechanics of fibre-reinforced sand. Geotechnique 60 (10), 791–799.

Verdugo, R., Ishihara, K., 1996. The steady state of sandy soils. Soils Found. 36 (2), 81–91.

Yetimoglu, T., Salbas, O., 2003. A study on shear strength of sands reinforced with randomly distributed discrete fibers. Geotext. Geomembranes 21 (2), 103–110.

Jakhongirbek Ganiev obtained his ME degree with a major in Geotechnical Engineering from Nagoya University in 2019. He is currently a PhD candidate in Geotechnical Engineering at Nagoya University. He is a member of the Japanese Society of Civil Engineers. His research interests cover the experimental investigation and testing of geomaterials with particular attention to sustainable ground improvement, constitutive modeling, and numerical analysis of geo-structures.